ACS OMEGA

http://pubs.acs.org/journal/acsodf

Article

Design and Development of Novel Glitazones for Activation of PGC-1α Signaling Via PPAR-γ Agonism: A Promising Therapeutic Approach against Parkinson's Disease

Prabitha Prabhakaran, Abhishek Nadig, Sahyadri M, Sunanda Tuladhar, Ruby Mariam Raju, Saravana Babu Chidambaram, Bettadaiah Bheemanakere Kempaiah, Nulgumnalli Manjunathaiah Raghavendra, and Prashantha Kumar BR*

Cite This: *ACS Omega* 2023, 8, 6825−6837

Read Online

ACCESS | Metrics & More | Article Recommendations | Supporting Information

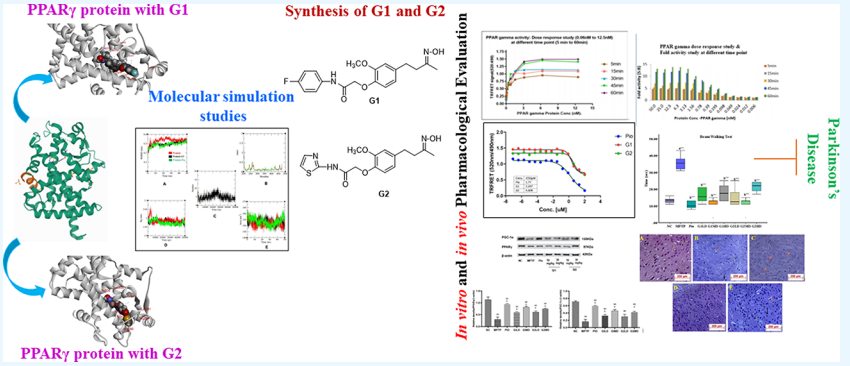

ABSTRACT: Herein, we rationally designed and developed two novel glitazones (G1 and G2) to target peroxisome proliferator-activated receptor-gamma coactivator 1-alpha (PGC-1α) signaling through peroxisome proliferator-activated receptors (PPAR)-γ agonism as a therapeutic for Parkinson's disease (PD). The synthesized molecules were analyzed by mass spectrometry and NMR spectroscopy. The neuroprotective functionality of the synthesized molecules was assessed by a cell viability assay in lipopolysaccharide-intoxicated SHSY5Y neuroblastoma cell lines. The ability of these new glitazones to scavenge free radicals was further ascertained via a lipid peroxide assay, and pharmacokinetic properties were verified using in silico absorption, distribution, metabolism, excretion, and toxicity analyses. The molecular docking reports recognized the mode of interaction of the glitazones with PPAR-γ. The G1 and G2 exhibited a noticeable neuroprotective effect in lipopolysaccharide-intoxicated SHSY5Y neuroblastoma cells with the half-maximal inhibitory concentration value of 2.247 and 4.509 μM, respectively. Both test compounds prevented 1-methyl-4-phenyl-1,2,3,6-tetrahydropyridine-induced motor impairment in mice, as demonstrated by the beam walk test. Further, treating the diseased mice with G1 and G2 resulted in significant restoration of antioxidant enzymes glutathione and superoxide and reduced the intensity of lipid peroxidation inside the brain tissues. Histopathological analysis of the glitazones-treated mice brain revealed a reduced apoptotic region and a rise in the number of viable pyramidal neurons and oligodendrocytes. The study concluded that G1 and G2 showed promising results in treating PD by activating PGC-1α signaling in brain via PPAR-γ agonism. However, more extensive research is necessary for a better understanding of functional targets and signaling pathways.

1. INTRODUCTION

Parkinson's disease (PD) is a progressive neurodegenerative ailment that affects about one percent of the world's elderly population. A higher incidence is observed with advancing age, primarily affecting the male population.[1,2] About 85% of the disease is sporadic and is characterized by α-synuclein aggregation, mitochondrial dysfunction, aberrations in the ubiquitin-proteasome system, and autophagy.[3] Environmental elements and susceptible genes are allied to the progression of sporadic PD.[4] Conversely, the mutations of either autosomal dominant or autosomal recessive genes contribute to familial PD.[5]

In PD, the lack of nigrostriatal dopamine transmission arises due to the degeneration of dopaminergic neurons of the substantia nigra pars compacta, and Lewy bodies are detected in the affected brain regions. It is well-established that factors

Received: November 24, 2022
Accepted: February 1, 2023
Published: February 10, 2023

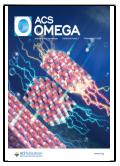

Scheme I. Synthesis of 4-(4-Hydroxy-3-methoxyphenyl)butan-2-one

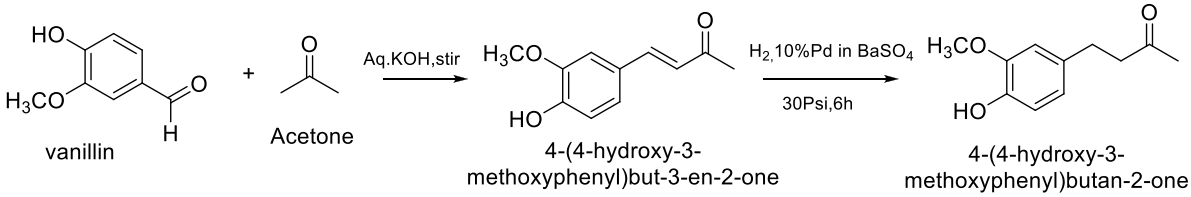

like oxidative stress, cellular dysfunction involving mitochondrial dysfunction, apoptosis, autophagy, and chronic neuroinflammation are interlinked with PD.[3,6,7] Thus, regulating oxidative stress and inflammation and preventing apoptosis is essential for treating this intricate and incapacitating condition.

Existing pharmacotherapy can only alleviate the symptoms but cannot control the progression of PD or eradicate the disease. The prevention and recovery of neuronal damage by peroxisome proliferator-activated receptor gamma (PPAR-γ) agonists are widely applied to develop numerous in vivo and in vitro models for various neurological disorders.[8−13] PPAR agonists can regulate numerous molecular pathways and stimulate gene expression during transcription, making them suitable for treating neurodegenerative diseases. The PPAR-γ agonists have displayed a wide range of activities in several experimental models that positively influenced the pathology of the diseases.[14−25] These molecules may provide neuroprotection by controlling the gene expression associated with processes significant for the neurons to survive. However, extensive investigations are required to assess the neuroprotective benefits and molecular mechanisms of PPAR-γ agonists. Numerous PPAR agonists, including rosiglitazone, pioglitazone, L-165041, GW-501516, GW0742, bezafibrate, fenofibrate, and MHY908 function at the transcriptional stage and are emerging as a neoteric potential therapeutic point of neurodegenerative diseases.[15−26]

The glitazones/thiazolidinediones scaffold has been successful in drug design and development to synthesize new lead molecules as they function as PPAR-γ agonists.[16] PPAR-γ receptors play a significant role in differentiating adipocytes, lipid, and carbohydrate metabolism by regulating the transcription of many genes.[18] In addition, they are present in macrophages, vascular smooth muscle cells, colonic epithelial cells, vascular endothelial cells, and renal glomerular cells—the glitazones treat diabetes by improving insulin sensitivity through PPAR-γ activation. The glitazones regulate genes related to insulin sensitivity and reduce insulin resistance by activating PPAR, the highly expressed receptors in insulin-sensitive organs, e.g., the pancreas, the substantia nigra, and the putamen in the brain. The glitazones activate proliferator-activated receptor gamma coactivator 1-alpha (PGC1-α), a mitochondrial regulator, thereby modulating mitoNEET, a mitochondrial membrane protein, and reducing oxidative stress and cell apoptosis in the long run. They reduce oxidative stress in neurons and improve mitochondrial function by inhibiting microglial activation. Moreover, the PGC1-α is the master gene involved in the biogenesis of mitochondria and has demonstrated neuroprotection in models of PD.[27]

Further, type 2 diabetes mellitus and Parkinson's patients share disruption in common mechanistic pathways, including mitochondrial dysfunction, autophagy, inflammatory response, and impaired glucose tolerance or insulin resistance. Recently, repurposing glitazones to prevent neurodegeneration in diabetic patients demonstrated that they can be considered a PD treatment option.[26] This article aims to design and synthesize novel glitazones targeting PPAR-γ-dependent PGC-1α signaling in neurons, thereby establishing a new therapeutic strategy for PD.

The use of glitazones has been successfully exploited to synthesize new lead molecules, as they act as PPAR-γ agonists. In the present study using molecular modeling, the binding affinity and interaction with PPAR-γ were evaluated. The glitazones were synthesized by optimizing synthetic protocols and characterized by NMR spectroscopy and mass spectrometry to confirm their molecular structures. Using a time-resolved fluorescence-Förster resonance energy transfer (TR-FRET) PPAR-γ competitive binding assay, the binding parameters were ascertained. Moreover, the potency of the synthesized molecules was evaluated in lipopolysaccharide (LPS)-induced SHSY5Y cell lines and to investigate the neuroprotective effects through neurobehavioral, neurochemical, and histopathological changes in the 1-methyl-4-phenyl-1,2,3,6-tetrahydropyridine (MPTP)-induced PD mice model. Therefore, this work aims at exploring the neuroprotective effects of newly synthesized G1 and G2 as individual lead molecules to treat PD and to study the various neuronal activation mechanisms involved.

2. RESULTS AND DISCUSSION

2.1. The Rational Design of Glitazones. The structure-based design of molecules is an effective way to select ligands. It provides insights into moieties present in the ligands, which may be modified to achieve molecules with enhanced activity and selectivity. Their characteristic property of PPAR-γ agonism can be linked to the application of glitazones as insulin sensitizers. The claim that glitazone molecules may have a therapeutic impact on parkinsonism may be backed by specific results obtained from animal model studies of Parkinson's disease, where rosiglitazone protected dopaminergic neurons in rodents[28,29] or pioglitazone improved parkinsonian syndrome in rhesus monkeys.[30]

The glitazones were designed to induce the changes in the conformation of the PPAR-γ and coactivators (the PGC-1α), considering that the mitochondrial biogenesis process might be upregulated by induced conformational changes at the PGC-1α binding domain and result in a neuroprotective effect. Considering the various side effects associated with the thiazolidinedione ring and in order to interact with PPAR-γ receptors, the structure of glitazones requires an aromatic trunk, lipophilic tail, acidic headgroup, and heteroatom spacer. In light of the above facts, we designed our glitazones to meet these structural requirements as well as the pharmacotherapeutic requirements.

2.2. Chemistry and Synthesis. A highly efficient and convenient synthetic protocol was followed to synthesize the target molecules as outlined in Schemes I−III. A cross-aldol condensation between vanillin and acetone, followed by a

https://doi.org/10.1021/acsomega.2c07521
ACS Omega 2023, 8, 6825−6837

Scheme II. Synthesis of Acylated Amines

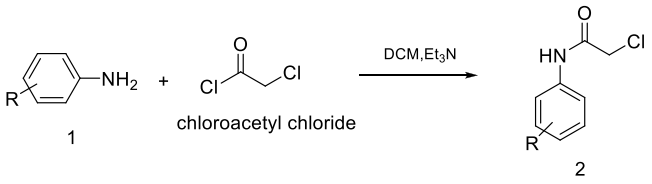

hydrogenation reaction in 10% $Pd/BaSO_4$ in ethanol at 30 Psi pressure, resulted in the compound zingerone. The reaction between chloroacetyl chloride and arylamine/alkyl amine in the presence of triethylamine led to Compound 2. Compound 2 and zingerone, upon refluxing in anhydrous K_2CO_3 for 24 h, resulted in a condensation product. The final products G1 and G2 were obtained via the oxime formation reaction between the condensation product and the hydroxylamine hydrochloride. The structures of various compounds elucidated by NMR and mass spectrometric studies are narrated below.

2.2.1. G1-(Z)-N-(4-Fluorophenyl)-2-(4-(3-(hydroxyimino)-butyl)-2-methoxyphenoxy)acetamide. Pale yellow solid. 283−285 °C. ^{1}H NMR (400 MHz, dimethyl sulfoxide (DMSO)) δ 1.072 (t, Ar−CH_2−CH_2−, 2H, J = 7.0 Hz), 2.073 (t, Ar−CH_2−CH_2−, 2H, J = 7.0 Hz), 2.867 (s, Ar-OCH_3-, 3H), 4.274 (s, Ar-OCH_2−, 2H), 6.951−6.952 (dd, H−Ar, 1H, J = 9.0 Hz, J = 3.0 Hz, J = 1.0 Hz), 7.010 (dd, H−Ar, 1H, J = 9.0 Hz, J = 3.0 Hz), 7.169 (dd, H−Ar/ortho-F, 2H, J = 9.0 Hz, J = 1.0 Hz), 7.450 (dd, H−Ar/meta-F, 2H, J = 9.0 Hz, J = 1.0 Hz), 10.909 (s, NH).

^{13}C NMR (400 MHz, DMSO) δ −2.085 (s, =C-CH_3), 17.225 (s, Ar−CH_2−CH_2-), 26.727 (s, Ar-CH_2−CH_2−), 65.016 (s, Ar−O-CH_3), 84.430 (s, -O-CH_2), 115.160 (s, C−Ar), 115.555 (s, C−Ar/ortho F), 121.862 (s, Ar-C-CH_2), 124.162 (s, -NH-C-Ar), 130.156 (s, C−Ar/meta F), 145.666 (s, C−Ar-O-CH_2), 145.676(s, C−Ar−OCH_3), 153.726 (s, C=NOH), 163.357 (d, F-C-Ar, J = 250.0 Hz), 173.732 (s, C=ONH). Exact mass calculated: 360.1479 (M+), $[M + H]^+$: 361.1558.

IR (V_{max}, cm^{-1}) 3509.5 (oxime −OH), 3426.6 (−NH stretch), 3138.4−3072.0 (aromatic −CH), 3056.3−2970.8 (−CH alkane), 2846.6 (−CH $_{stretch}$), 2920.1 (−CH alkane stretch), 2956.3−2846.6 (−CH alkane), 1745.3 (-C=O stretch), 1714.3 (-C=N−OH, stretch), 1603.4−1482.0 (C=C aromatic), 1479.8−1456.4 (−CH_3 alkane), 1447.1 (−NH), 1443.6−1121.6 (−CH), 1482.4 (C−F stretch).

2.2.2. G2-(Z)-2-(4-(3-(Hydroxyimino)butyl)-2-methoxyphenoxy)-N-(thiazol-2-yl)acetamide. Yellow solid, 225−228 °C. ^{1}H NMR (400 MHz, DMSO) δ 0.367 (s, =C−CH_3, 3H), 1.072 (t, Ar-CH_2-CH_2−, 2H, J = 7.0 Hz), 2.073 (t, Ar−CH_2−CH_2−, 2H, J = 7.0 Hz), 2.867 (s, Ar-OCH_3-, 3H), 4.274 (s, Ar-OCH_2−, 2H), 6.951−6.952 (dd, H−Ar, 1H, J = 9.0 Hz, J = 3.0 Hz, J = 1.0 Hz), 7.010 (dd, H−Ar, 1H, J = 9.0 Hz, J = 3.0 Hz), 7.494 (d, Ar−H, 1H, J = 9.0 Hz), 8.398 (d, Ar−H, 1H, J = 9.0 Hz), 10.909 (s, NH).

^{13}C NMR (400 MHz, DMSO) δ −2.085 (s, =C-CH_3), 17.225 (s, Ar−CH_2−CH_2-), 26.727 (s, Ar-CH_2−CH_2−), 65.016 (s, Ar−O-CH_3), 84.430 (s, -O-CH_2), 115.160 (s, C−Ar), 121.108 (s, Ar-C), 121.862 (s, Ar-C), 133.988 (s, Ar-C-NH), 145.676 (s, H-C-N), 145.666 (s, Ar−C−O-CH_2),

Scheme III. Synthesis of Glitazones

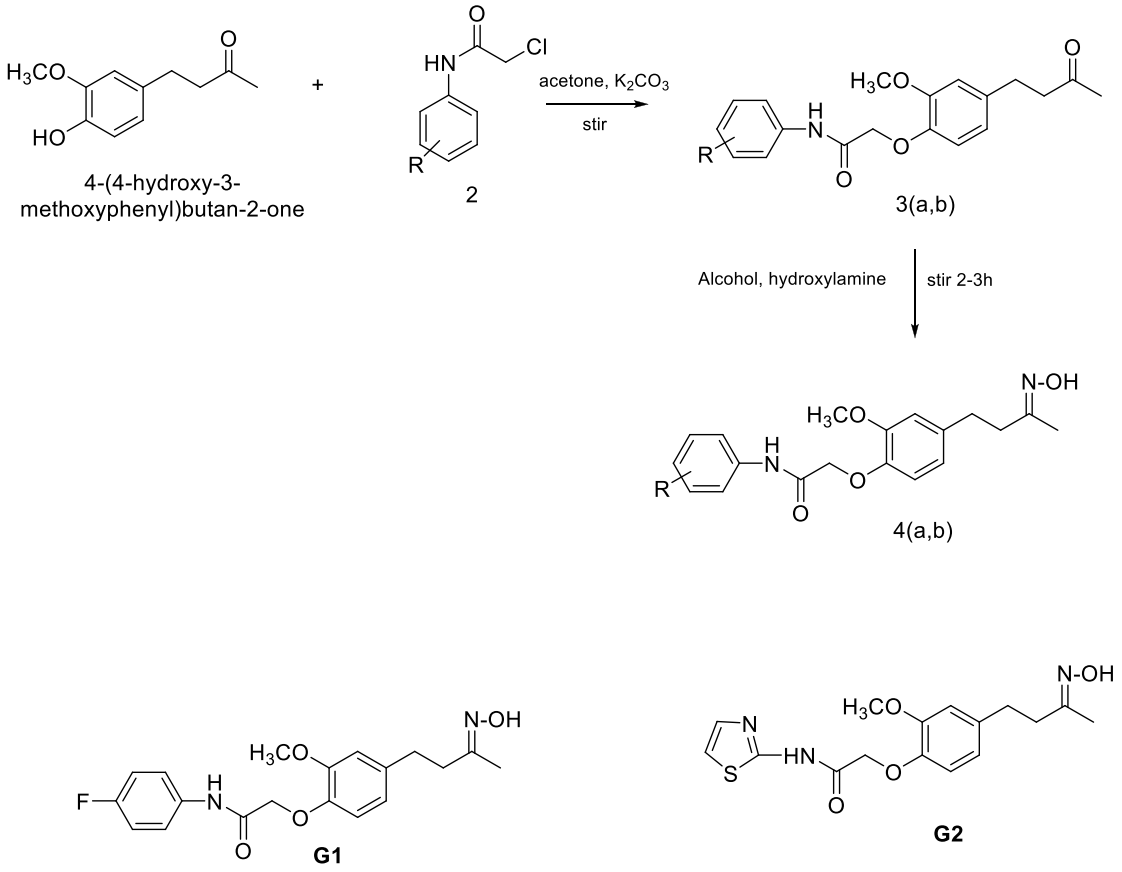

https://doi.org/10.1021/acsomega.2c07521
ACS Omega 2023, 8, 6825−6837

Table 1. In Silico ADMET Properties of Synthesized Glitazones[a]

Cpd No	Solubility	BBB	CYP2D6	Hepatotoxic	HIA	NTP Carcinogen	Ames Mutagenicity	Rat oral LD 50 (g/kg body weight)
G1	3	3	Noninhibitor	Nontoxic	0	Noncarcinogenic	Nonmutagenic	2.81
G2	3	3	Noninhibitor	Nontoxic	0	Noncarcinogenic	Nonmutagenic	2.39

[a]BBB: Blood-brain barrier; CYP2D6: Cytochrome P450 2D6; HIA: Human intestinal absorption; NTP: National Toxicology Program.

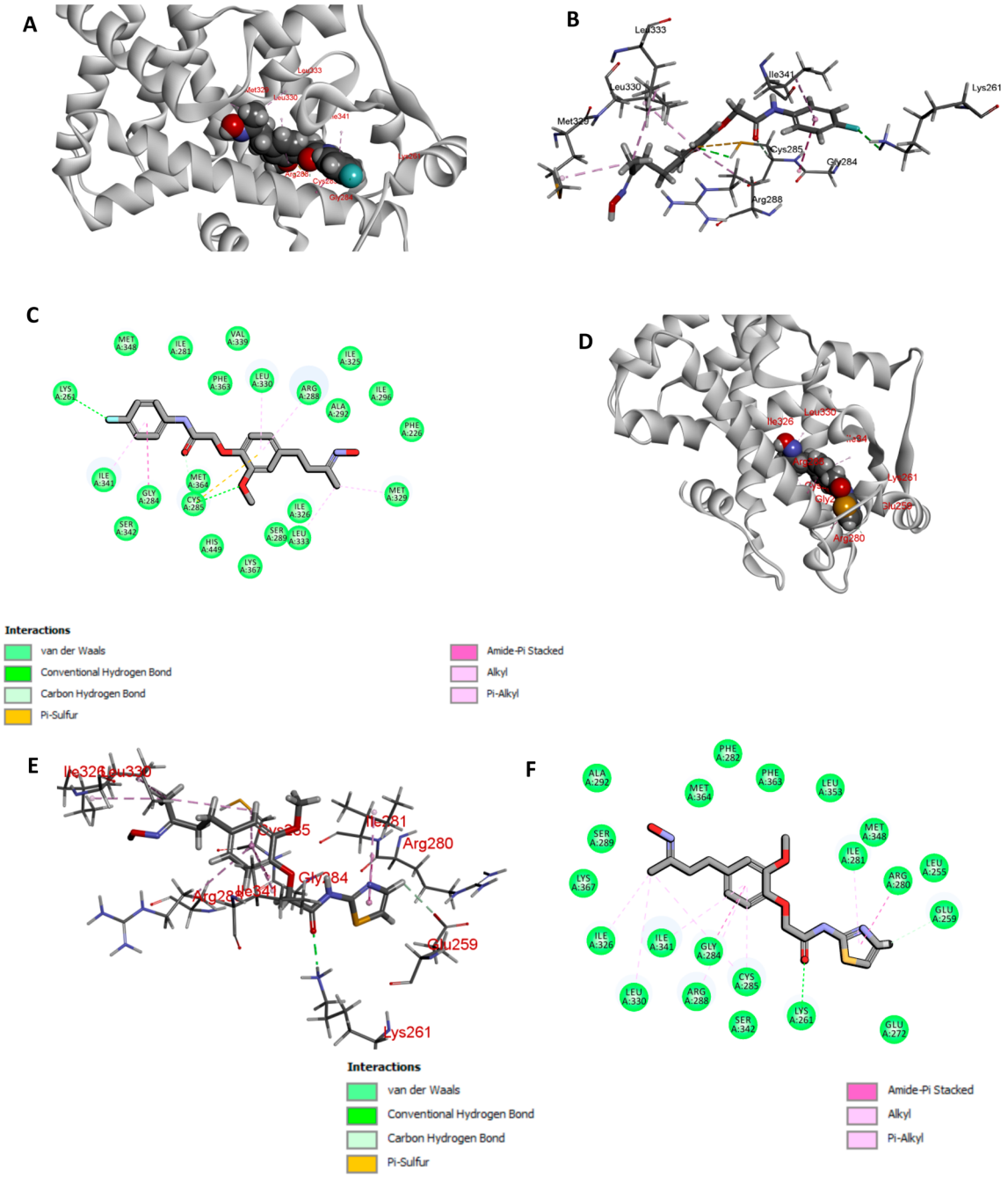

Figure 1. Docked conformations of (A) synthesized glitazone G1, (B, C) the interacting residues surrounding G1, (D) synthesized glitazone G2, and (E, F) the interacting residues with the PPAR-γ protein (3CS8).

145.676 (s, Ar−C−OCH_3), 153.726 (s, **C**=NOH), 173.732 (s, **C**=ONH). Exact mass calculated: 349.1090 (M+), $[M + H]^+$: 350.1169.

IR (V_{max}, cm^{-1}) 3498.1 (oxime −OH), 3422.6 (−NH), 3189.6−3090.7 (=C−H aromatic), 3102.4−3090.0 (−C-H), 3040.4−2847.6 (−CH alkane), 1781.6 (C=O), 1791.1 (Oxime), 1606.3, 1087.4 (C=N), 1596.3−1476.8 (=CH), 1473.0−1384.4 (−CH), 1365.4 (N−H), 626.9−568.2 (C−S stretch).

2.3. The Molecular Mechanism for Activation of PPAR-γ with PGC-1α. The synthesized glitazones screened for absorption, distribution, metabolism, excretion, and toxicity (ADMET) were nontoxic to liver cells. Moreover, they were established as noncarcinogenic and nonmutagenic (Table 1),

https://doi.org/10.1021/acsomega.2c07521
ACS Omega 2023, 8, 6825−6837

Table 2. Interacting Amino Acid Residues Obtained from Docking Analysis of the Synthesized Glitazones G1 and G2 with PPAR-γ Protein

	G1	G2
Interacting Residues	Phe 226, Lys 261, Ile 281, Gly 284, Cys 285, Arg 288, Ser 289, Ala 292, Ile 296, Ile 325, Met 329, Leu 330, Leu 333, Val 339, Ile 341, Ser 342, Met 348, Phe 363, Met 364, Lys 367, His 449	Leu 255, Glu 259, Lys 261, Glu 272, Arg 280, Ile 281, Gly 284, Cys 285, Arg 288, Ser 289, Ala 292, Ile 326, Leu 330, Ile 341, Ser 342, Met 348, Leu 353, Phe 363, Met 364, Lys 367

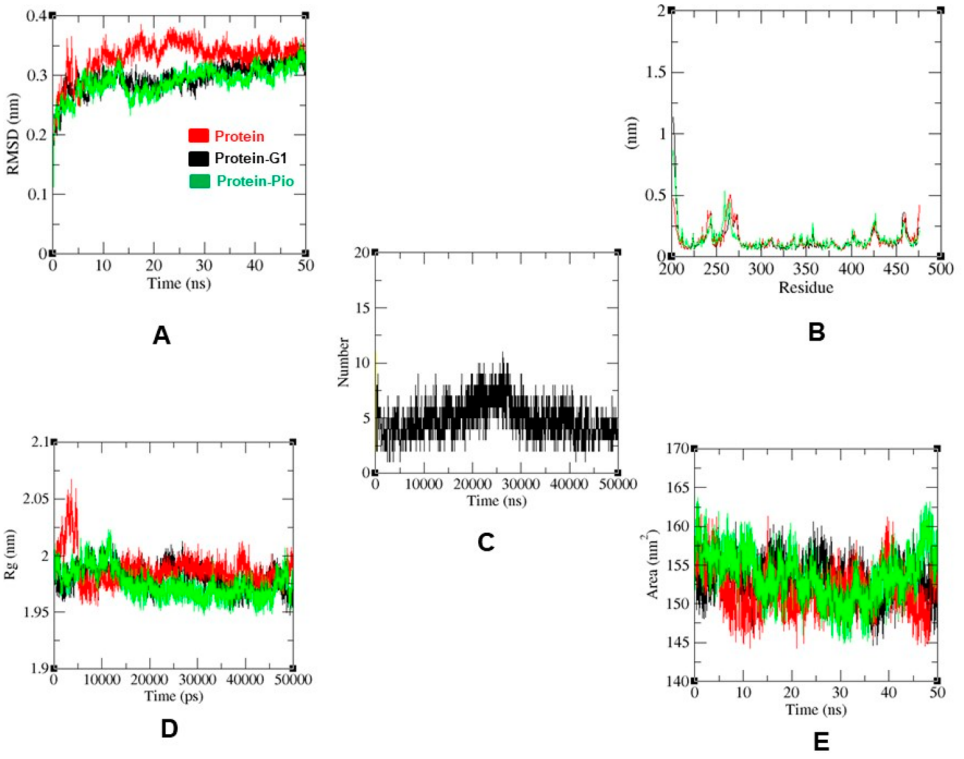

Figure 2. (A) RMSD; (B) RMSF profiles; (C) number of H-bonds; (D) radius of gyration; (E) SASA of the PPAR-γ protein and G1 obtained using MD simulation.

as reflected in carcinogens and ames mutagen. As reported in the literature, the glitazones/thiazolidinediones (TZDs) acting as PPARγ agonists initiate a configurational change inside the PPAR, which leads to the detachment of the corepressor amino acid chain. The coactivator amino acid chain then participates in the target gene transcription. Thiazolidinediones act via PPARs, which depend on transcriptional coactivators such as PGC-1α. Decreased PGC-1α levels cause mitochondrial dysfunctions with increased oxidative stress commonly associated with many neurodegenerative disorders.[31]

The molecular docking studies recognized the interaction pattern of the synthesized glitazones with PPAR-γ. G1 and G2 have −35.1081 and −49.1987 kcal/mol CDOCKER interaction energies (docking scores), respectively. These findings suggested that G2 interacts more strongly with PPAR-γ protein than G1.

The docked conformations of the glitazone complexes are shown in Figure 1, and the interacting residues of the PPAR-γ protein are shown in Table 2. Figure 1 depicts that a couple of hydrophobic residues surrounded G1 and G2, and Lysine 261 participated in forming a conventional hydrogen bond. The docking analysis illustrated that hydrophobic forces and hydrogen bonding dominated the interaction.

2.4. Molecular Dynamics Studies. Molecular dynamics (MD) simulations of PPAR-γ complexes provided a detailed insight into the dynamics of protein−ligand interactions that resulted in a stable bound conformation and visualized how ligand binding changed the protein conformations. The root-mean-square deviation (RMSD) and gyration of backbone atoms were plotted against a 50 ns time scale throughout the trajectory. The RMSD plots in Figure 2A illustrated that the RMSD of apoprotein increased above 0.4 Å, while when complexed with candidate molecule, RMSD converged at less than 0.3 Å. Further, the deviation in the lead molecules was less than 0.5 Å during MD simulations. This indicated that the complex PPAR-γ bound to PGC-1α protein was stabilized in the presence of candidate molecule G1.

The parameters, including the root, mean square fluctuation, the number of intermolecular hydrogen bonds (H-bonds, n), and solvent accessible surface area (SASA), reflected the stability and dynamic behavior of the docked G1-PPAR complex in a solvated state for 50 ns (Figure 2). Collectively, these simulations provided more profound insight into the compactness of protein, the surface of protein available to the solvent, complex stability, and protein residue flexibility that indicated the formation of a stable G1-PPAR-γ complex.

2.5. In Vitro Evaluation of the Synthesized Glitazones. *2.5.1. TR-FRET PPAR-γ Competitive Binding Assay.* The Lantha screen (time-resolved fluorescence) competitive binding assay screened the synthesized compounds for their PPAR-γ binding affinity. The assay was sensitive and accurate in determining the binding affinity of the synthesized

https://doi.org/10.1021/acsomega.2c07521
ACS Omega 2023, 8, 6825−6837

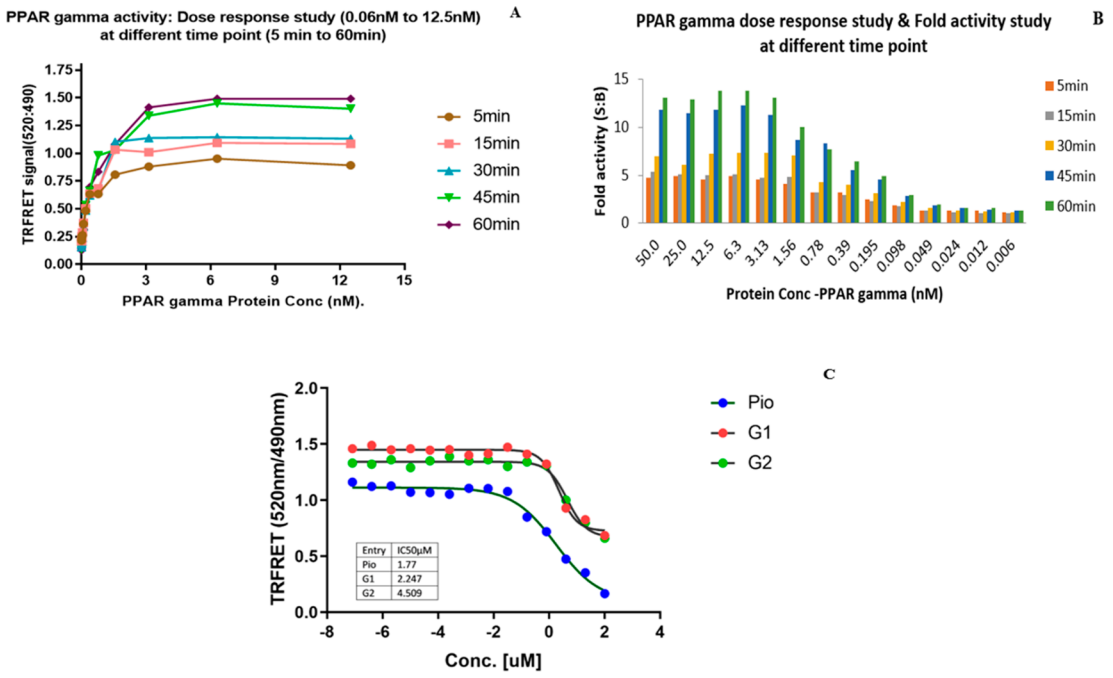

Figure 3. Lantha screen TR-FRET PPAR-γ competitive binding assay to assess the potency of synthesized compounds G1 and G2 and standard drug pioglitazone (A) Dose−Response study of PPAR-γ protein. (B) The fivefold activity study at different time point intervals; (C) IC_{50} of the synthesized compounds (G1 and G2) and the reference compound.

compounds. The fluorescence energy transfer from the terbium-labeled antibody to the tracer occurred in Fluormone Pan-PPAR Green bound PPAR-γ with a high time-resolved fluorescence resonance energy transfer (TR-FRET) ratio. The synthesized compounds interacted with PPAR-γ competitively, interrupting the FRET between the tracer and the antibody. The 520 nm/495 nm TR-FRET ratio was measured at room temperature upon incubation to ascertain the half-maximal inhibitory (IC_{50}) value. Figure 3C illustrates the decrease in the TR-FRET emission ratio, a measure of relative PPAR-γ affinities. The assay results indicated that the IC_{50} value for G1, G2, and standard drug pioglitazone were 2.247, 4.509, and 1.77 μM, respectively (Figure 3). The results showed that the compounds exhibited a binding affinity to the target protein that was similar to each other but different from that of the standard pioglitazone. The results suggested that the synthesized glitazones interacted with PPAR-γ with a moderate binding affinity.

2.5.2. In Vitro Evaluation of Neuroprotection of the Synthesized Glitazones in the LPS-Induced SHSY5Y Cell Lines. The 3-[4,5-dimethylthiazol-2-yl]-2,5 diphenyl tetrazolium bromide (MTT) assay determined the IC_{50} values for the synthesized glitazones G1 and G2 and evaluated the in vitro neuroprotection against LPS-stimulated inflammatory incidents in SHSY5Y cell lines. Both G1 and G2 showed lower IC_{50} values of 39.46 ± 3.81 and 40.23 ± 0.11 μM, respectively, as compared with standard pioglitazone (42.86 ± 0.33 μM), indicating better potency at lower concentrations and lower systemic toxicity when applied to the patient.[32]

2.6. In Vivo Evaluation. *2.6.1. Acute Oral Toxicity Study.* The compounds G1 and G2, tested at 300 mg/kg, did not exhibit any clinical signs of acute toxicity or mortality (Table 3) (Figure S7) and were considered safe. Consequently, neuroprotective evaluations with novel synthesized glitazones

Table 3. Results of Oral Toxicity Study

Group of Treatment	Dose (μg kg^{-1})	Lethality	Signs of Toxicity
Control		0/6	
G1	2000	2/3	hyperactivity, irritability, convulsions, and massive change in weight
G1	300	0/3	
G2	2000	2/3	hyperactivity, irritability, convulsions, and massive change in weight
G2	300	0/3	

were conducted with 1/3, 1/10, and 1/20 of the 300 mg/kg, i.e., ∼100 mg, 30 mg, and ∼10 mg/kg, respectively.

2.6.2. The Neurobehavioral Study by Beam Walk Test. The time to cross the narrow beam by the mice after the MPTP induction is presented in Figure 4. The test compounds (G1 and G2) significantly ($p < 0.001$) prevented the motor impairment induced by MPTP treatment. The G1MD (30 mg/kg) and G2MD (30 mg/kg) plus MPTP prevented the rise of total errors induced by the treatment with MPTP and crossed the narrow beam in a shorter duration of time when compared to the MPTP-injected group (Figure 4). Both G1 and G2 were more potent than the standard, as reflected in the reduced time for the treated animals. The synthesized glitazones improved the neurological and neurobehavioral alterations in the treated mice. Our behavioral findings are in agreement with those of earlier reports.[6,7,33]

2.7. Neurobiochemical Estimation. *2.7.1. Effect of G1 and G2 on MDA and GSH Levels in the Mice Brain.* The MDA level was estimated to evaluate the extent of oxidative damage to lipids and the neuroprotection by the test compounds. The MPTP-induced mice significantly ($p < 0.001$) increased the MDA level when compared to the control. G1 (30 mg/kg), G2 (30 mg/kg), and standard pioglitazone treatment followed by MPTP administration significantly prevented ($p < 0.001$) the apparent increase of

https://doi.org/10.1021/acsomega.2c07521
ACS Omega 2023, 8, 6825−6837

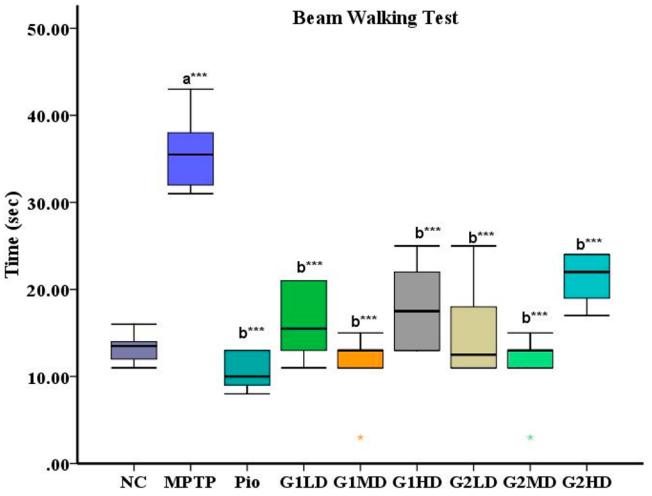

Figure 4. Effect of G1 and G2 on beam walk test enzymes. Data are expressed as mean ± SEM (n = 6). Significant difference * p < 0.05, ** p < 0.01, *** p < 0.001. (a) Significant when compared to normal control. (b) Significant when compared to the MPTP group.

the MDA level in the brain as compared to the MPTP-induced group (Figure 5D). Similarly, the MPTP administration significantly (p < 0.001) lowered the GSH levels compared to the control group (Figure 5A). However, treatment with test compounds G1 and G2 significantly (p < 0.001) restored the GSH levels when compared to MPTP group. The results obtained are in agreement with the previous results, where cholinergic acid supplementation upregulated the endogenous antioxidant enzyme activities in an MPTP-intoxicated mouse model.[33,34] The use of pioglitazone is supported by another study by Chang et al., which concluded that pioglitazone is a promising agent for reducing the incidence of PD in patients prediagnosed with diabetes mellitus. The drug also worked synergistically with statins, thereby improving its potential efficacy.[35]

2.7.2. Effect of G1 and G2 on CAT and SOD Levels in the Mice Brain. The antioxidant enzyme activity CAT and superoxide dismutase (SOD) levels were estimated to determine the beneficial effects of test compounds caused by MPTP treatment. There is a significant (p < 0.001) increase in CAT and SOD levels in the brain of MPTP-induced mice as compared to those of the control group, whereas mice treated with the standard pioglitazone, G1, and G2 exhibited a significant (p < 0.001) upsurge in antioxidant CAT and SOD levels in the brain when compared to MPTP-treated animals (Figure 5). The increase in oxidative damage lowers the activity of intracellular antioxidant enzymes like CAT and SOD. The reduced activity of SOD and CAT in MPTP mice might have resulted from the inactivation of the enzymes by H_2O_2. However, the test compounds G1 and G2 showed a positive effect on SOD and CAT activity and also restored GSH and MDA levels, thereby demonstrating the antioxidant

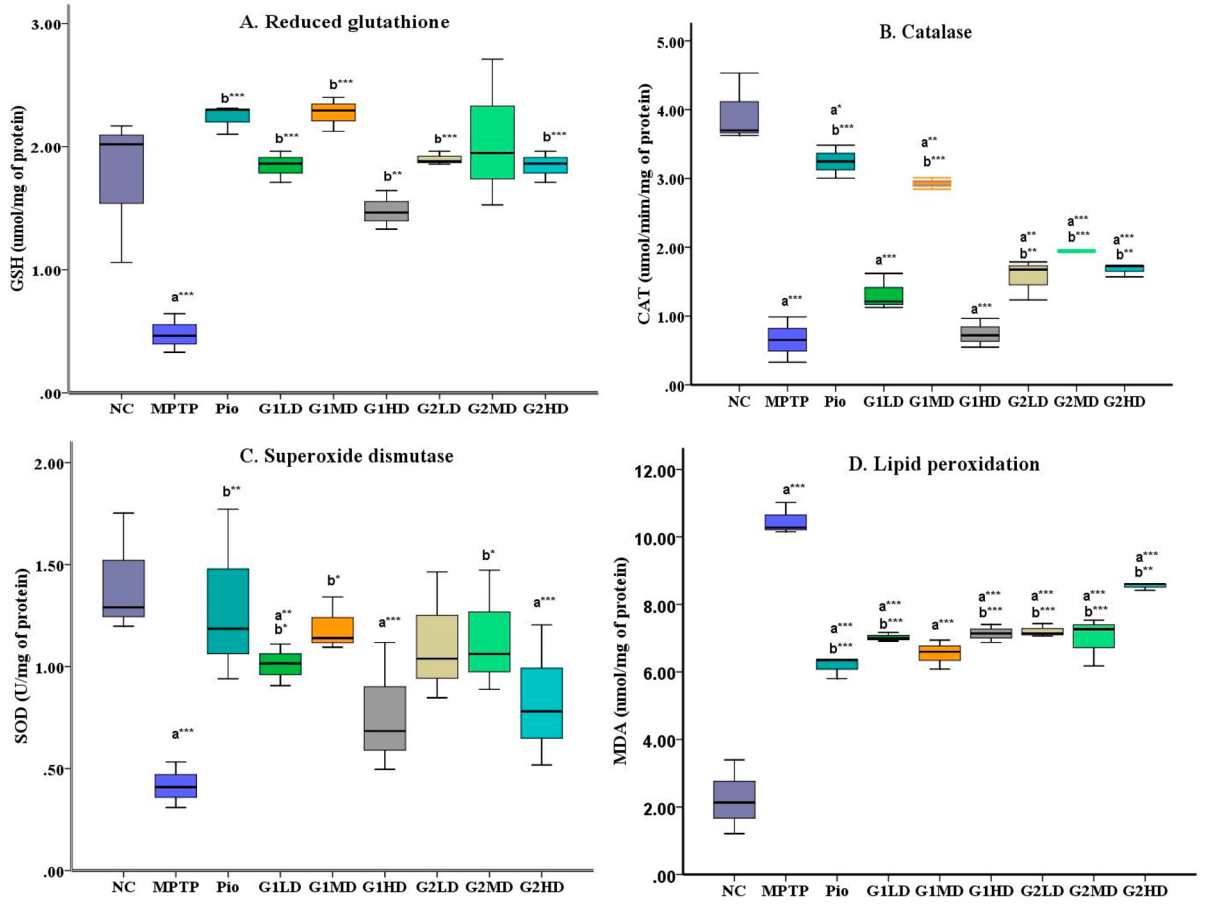

Figure 5. Effect of G1 and G2 on endogenous antioxidant enzymes. (A) GSH, (B) CAT, (C) SOD, (D) TBARS. Data are expressed as mean ± SEM, (n = 6). Significant difference * p < 0.05, ** p < 0.01, *** p < 0.001. (a) Significant when compared to normal control. (b) Significant when compared to the MPTP group.

https://doi.org/10.1021/acsomega.2c07521
ACS Omega 2023, 8, 6825−6837

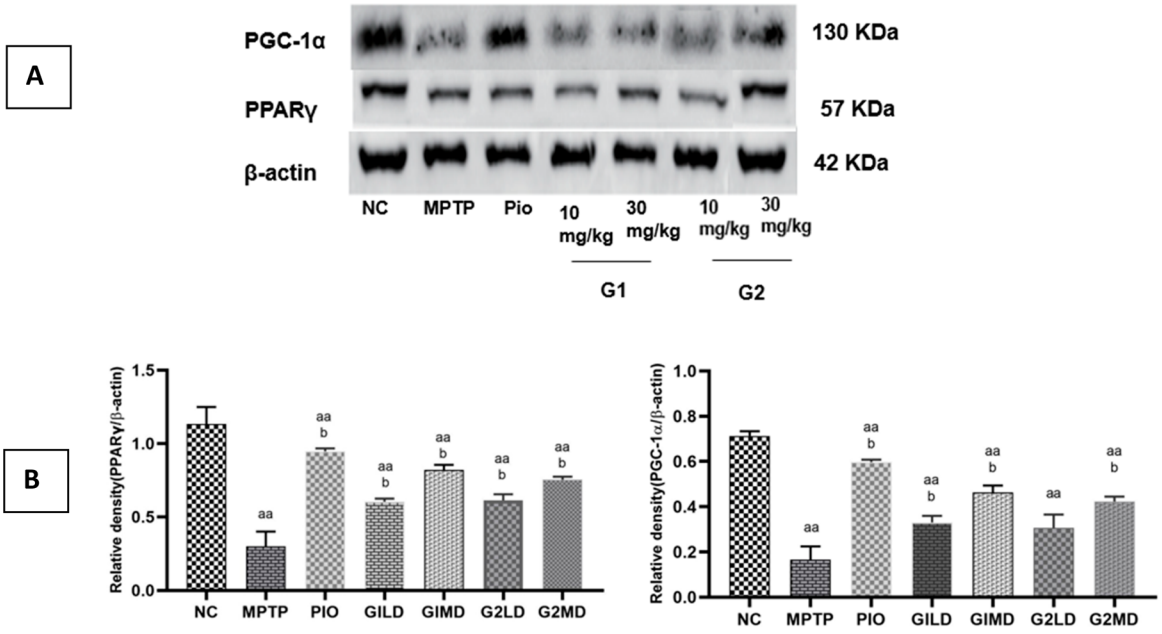

Figure 6. Comparative efficacy of G1 and G2 compounds in modulating the expression of PGC-1α and PPAR-γ compared to the effect of pioglitazone (a positive control) in "PD-induced models." Data are expressed as mean ± SEM, (n = 3). Significant difference $p < 0.05$. (aa) Significant when compared to the normal control. (b) Significant when compared to the MPTP group. A significant upregulation of the expression of PGC-1α and PPAR-γ was observed in the groups treated with G1 and G2 compared to the control as indicated by (A) western blot analysis to monitor the expression of PGC-1α and PPAR-γ from the brain sections of diseased and treated mice. (B) Bar diagram representing the levels of PGC-1α and PPAR-γ in western blot results.

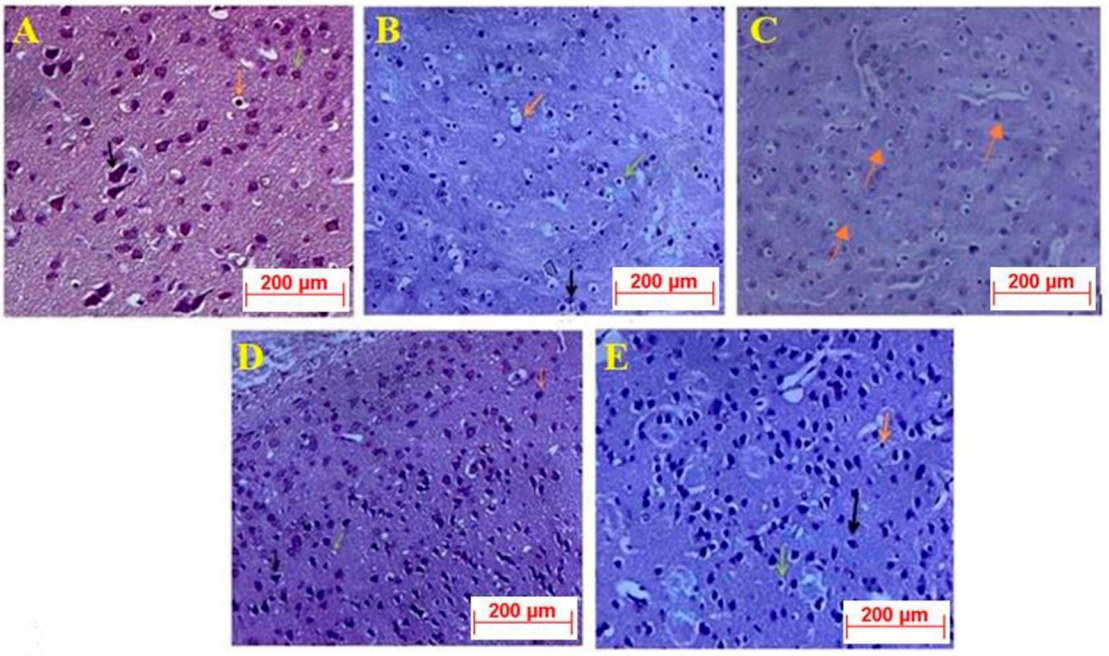

Figure 7. Histopathology images of substantia nigra region—The black arrow represents the healthy neurons. The orange arrow and green arrow represent degenerated neurons. (A) Normal control (100X), (B) MPTP (100X), (C) Pioglitazones (100X) 40 mg/kg bwt, (D) G1 (100X) 30 mg/kg bwt, (E) G2 (100X) 30 mg/kg.

efficacy of test compounds. The results obtained are in agreement with the previous evidence, where ursolic acid increased the endogenous antioxidant CAT and SOD enzyme activities in rotenone-induced Parkinsonism in mouse model.[3]

2.8. Western Blot Analysis of the Brain Sections of Mice. The brain sections of MPTP-induced mice, i.e., diseased mice, showed less intense bands, indicating lower PGC1-α and PPAR-γ levels. As evident from Figure 6, the treatment with the synthesized glitazones G1 and G2 resulted in significant upregulation of PGC1-α and PPAR-γ expression compared to the MPTP-treated group and has shown a similar effect as that of the standard pioglitazone group.[36]

2.9. Histopathological Studies. Cresyl violet staining was used to stain Nissl granules in order to indirectly measure the

https://doi.org/10.1021/acsomega.2c07521
ACS Omega 2023, 8, 6825−6837

neurodegeneration in tissue. MPTP administration significantly increased the degenerated neurons in substantial nigra, whereas Pioglitazone, G1, and G2 significantly ($p < 0.001$) reduced the degenerated neurons in substantial nigra as compared with the MPTP-treated group (Figures 7 and 8).

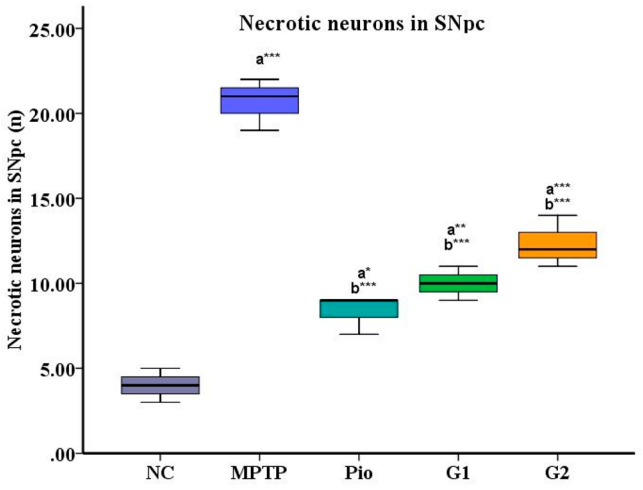

Figure 8. Effect of G1 and G2 on necrotic neurons in SNPc. Data are expressed as mean ± SEM ($n = 3$). Significant difference * $p < 0.05$, ** $p < 0.01$, *** $p < 0.001$. (a) Significant when compared to normal control. (b) Significant when compared to MPTP.

2.9.1. Estimation of the Neurotransmitter Dopamine. The MPTP animal showed a significant ($p < 0.001$) decrease in dopamine level when compared to the normal control, whereas pioglitazone, G1, and G2 exhibited a significant ($p < 0.001$) increase in dopamine level when compared to the MPTP group (Figure 9).[37]

3. MATERIAL AND METHODS

3.1. Molecular Docking for Rational Design of Glitazones for Activation of PGC-1α. The CDOCKER algorithm is a grid-based docking procedure that uses molecular dynamics simulation to dock molecules to a protein binding site. CDOCKER docking protocol in Discovery Studio 2019 was used for molecular docking, which involved adding a CHARMm force field to protein and ligand.[38−40] The protein prepared for the molecular docking studies was downloaded from the RCSB protein databank (PDB_ID: 3CS8 with 2.3 Å resolution).[41] The three-dimensional (3D) protein PPAR-γ bound to the PGC-1α peptide, and rosiglitazone had some missing regions at the Lys263-Thr268 residues. The missing region was reconstructed by homology modeling using SWISS MODELER online tools (https://swissmodel.expasy.org/) and PDB_ID: 3CS8 as a template structure. All water molecules from the crystal structure were removed to yield the protein file. The ligand molecules were prepared by adding CHARMm force fields, and these molecules were used for molecular docking. The final docked conformation was chosen based on the protein−ligand interactions and molecule orientation.

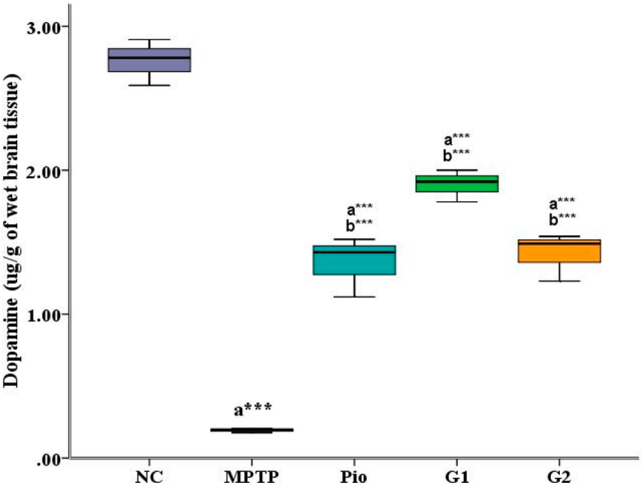

Figure 9. Concentration of dopamine in μg/g wet weight in brain homogenate. Data are expressed as mean ± SEM ($n = 6$). Significant difference * $p < 0.05$, ** $p < 0.01$, *** $p < 0.001$. (a) Significant when compared to the normal control. (b) Significant when compared to the MPTP group.

3.2. Molecular Docking (MD) and Simulation. MD simulations were conducted on the Ubuntu 16.04.7 platform with GROMACS 5.1.5 using the CHARMm27 force field.[42,43] Using the TIP3P water model, the protein alone and the ligand-protein complex were virtually positioned in a triclinic box. The counterions (Na^+/Cl) neutralized the system, and the steepest descent algorithm with a tolerance of 1000 kJ/mol/nm reduced the energy to a minimum. The number of particles, volume, and temperature (NVT) and the number of particles, pressure, and temperature (NPT) ensembles equilibrated the system for 200 ps, which was then subjected to a 50 ns MD production run with a 2 fs time step. Using the basic GROMACS analysis tools, the trajectories were stored, and numerous parameters were evaluated to determine the stability of complexes in a dynamic environment.

3.3. Synthesis and Characterization. The reagents and chemicals were procured from Merck and TCI Chemicals. Thin-layer chromatography (TLC) monitored the chemical reactions, and column chromatography purified the synthesized glitazones. The Bruker 400 MHz, FT NMR spectrophotometer recorded ^{1}H NMR and ^{13}C NMR spectra in deuterated dimethyl sulfoxide (DMSO-d_6) with tetramethylsilane (TMS) as an internal standard (δ ppm). An LC-MS ACQUITY UPLC mass spectrometer recorded mass spectra via electrospray (ES) ionization at 70 eV and time-of-flight detector.

3.3.1. Synthesis of 4-(4-Hydroxy-3-methoxyphenyl)-but-3-en-2 one) (Dehydrozingerone). The first step was the synthesis of 4-(4-hydroxy-3-methoxyphenyl)-but-3-en-2-one) through acetone via a cross-aldol condensation between vanillin and acetone, which involved an addition of 250 mL of acetone and aqueous potassium hydroxide (18.41g in 180 mL of water, 0.32 mol) to the vanillin solution in acetone (20g, 0.13 mol). The reaction continued at room temperature with continuous stirring until it was completed. TLC monitored the progress of the reaction with 20% ethyl acetate in the petroleum ether system. After the reaction, the mixture was acidified with 10% aqueous hydrochloric acid and extracted with dichloromethane (100 mL × 3). The extract was dried, filtered, and concentrated over anhydrous Na_2SO_4 and further refined using column chromatography on silica gel (100−200 mesh) to achieve the pure yellow crystalline component (20 g, 80%).

3.3.2. Synthesis of Vanillylacetone/Zingerone. Pd/$BaSO_4$ (10 mol percent) was added to a solution of dehydrozingerone (2 g, 10 mmol) in ethanol and hydrogenated for 6 h at 30 Psi

https://doi.org/10.1021/acsomega.2c07521
ACS Omega 2023, 8, 6825−6837

pressure. The reaction mixture was filtered upon completion of the process. The crude product was obtained by concentrating the organic layer, which was then refined using column chromatography on silica gel (200−400 mesh) to afford the pure yellow chemical (1.7 g, 85%).

3.3.3. Synthesis of 2-Chloro-N-substituted Acetamide. A dropwise addition of 2-chloroacetyl chloride (0.11 M) was done to a solution comprising arylamine/alkyl amine (0.1 M) and triethylamine (0.1 M) in dichloromethane (80 mL) at 0 °C. The solution was cooled to ambient temperature, and the reaction proceeded overnight with TLC monitoring. Ice-cold water was added to the resulting solution to separate the organic layer, which was passed through anhydrous Na_2SO_4. The crude product was distilled under reduced pressure and subsequently crystallized in a mixture of methanol and water.

3.3.4. Condensation of 2-Chloro-N-substituted Acetamide with Zingerone. 2-Chloro-*N*-substituted acetamide (0.01 M), zingerone (0.011 M), and finely powdered anhydrous potassium carbonate (0.02 M) were dissolved in anhydrous acetone (30 mL). The solution was allowed to cool to room temperature after it was refluxed for 24 h. TLC was used to monitor the reaction mixture until the reaction was completed. The solution was filtered, evaporated, and crystallized using a dimethylformamide-ethanol mixture.

3.3.5. Synthesis of Substituted Zingerone Oxime. To the solution of the condensation product of 2-chloro-*N*-substituted acetamide with zingerone (0.3 g) in ethanol (20 mL), the hydroxylamine hydrochloride (0.96 g) and potassium carbonate were added. The reaction continued at room temperature with stirring until completion and was monitored by TLC using 20% ethyl acetate in petroleum ether. The reaction mixture was filtered upon completion, and the crude product was thoroughly washed with ethanol (10 mL). The filtrate was concentrated and extracted in dichloromethane (10 mL). The organic layer was dried over anhydrous Na_2SO_4 and concentrated into a pure white crystalline substance.

3.4. In Vitro Evaluation of Novel Glitazones. TR-FRET PPAR-γ competitive binding assay for high-throughput screening of ligands for PPAR-γ was performed to ascertain the binding parameters of the synthesized glitazones. The detailed procedure is included in the Supporting Information S12.
In vitro studies on synthesized glitazones using LPS-induced SHSY5Y cell lines was performed using the procedure included in Supporting Information S12.

3.5. In Vivo Evaluation of Novel Glitazones. Ethics statement procedure included in Supporting Information S13.[44]

3.5.2. Acute Oral Toxicity Study. The acute oral toxicity was conducted for newly produced novel glitazones compounds following the OECD 423 guidelines C25 and C34.[45] The tests were done with 300 and 2000 mg/kg since there were no toxicity indications like irritability, hyperactivity, massive weight change, convulsions, or death at the doses of 5 and 50 mg/kg.

3.5.3. Groups and Treatment for Mice Model of PD. The animals were placed into nine groups, each with six animals. Parkinson's disease was induced by an intraperitoneal administration of MPTP (Table S3 shown in Supporting Information). Except for the normal control, all the experimental animals were injected with MPTP 80 mg/kg bwt (2 × 40 mg/kg bwt at 16 h intervals). Treatment was given for 5 days; the test compounds were administered orally, and the animals were euthanized after the study.

3.5.4. The Neurobehavioral Study by Beam Walk Test. The beam walk test was carried out using a modified version of the conventional procedure.[46] Before being administered with MPTP, mice were trained to cross a tight beam of 100 cm in length to reach an enclosed escape platform. To create an avertable stimulus and motivate the mice to transit the narrow beam to the dark and confined goal box, bright light (20 lx) was positioned above it. The mice were housed separately at the start of the beam after being injected with MPTP. The time taken by mice to cross the beam, the total number of foot slips, and the time they were immobile were documented. A maximum of 60 s was allowed for the mice to cross the beam. The treatment groups were unknown to the observer who rated the mice's behavior.

3.6. Neurobiochemical Estimation: Estimation of Antioxidant Enzymes. The brains were homogenized in sodium phosphate buffer with a fast prep-24 tissue homogenizer and centrifuged at 4000 rpm for 10 min. The supernatant collected was used to estimate SOD, reduced GSH, CAT, and bars. Further, the protein concentration was determined by Lowry's method.[47,48]

3.6.1. Measurement of Superoxide Dismutase.[47] A 0.3 mL sodium pyrophosphate buffer (0.025 M, pH 8.3) was added to 0.05 mL of homogenate, followed by the addition of 0.025 mL of 5-methylphenazin-5-ium methyl sulfate (PMS,186 μM) and 0.075 mL of nitro blue tetrazolium (NBT), 300 μM in buffer, pH 8.3. Next, 0.075 mL of nicotinamide adenine dinucleotide (NADH) was added and incubated at 30 °C for 90 s. Glacial acetic acid (0.25 mL) was added to quench the reaction, followed by vigorous shaking with *n*-butanol. The mixture was then centrifuged for 1 min at 4000 rpm. The colorimetric analysis was done at 560 nm using *n*-butanol (1.5 mL) as a blank.

3.6.2. Measurement of Reduced Glutathione. As per the method by Jollow et al., an equivalent volume of ice-cold trichloroacetic acid (5%) was combined with 0.25 mL of brain homogenate (TCA) to measure glutathione.[49] The precipitate was removed, and the supernatant was recovered following centrifugation for 10 min at 3000 rpm. 0.25 mL of 0.2 M phosphate buffer (pH 8.0) and 0.5 mL of 5,5-dithio-bis(2-nitrobenzoic acid) (DTNB) (0.6 mM in 0.2 M phosphate buffer, pH 8.0) were added to a 1 mL aliquot of supernatant and thoroughly mixed. The absorbance was measured at 412 nm using a spectrophotometer (UV, Shimadzu, Japan).

3.6.3. Measurement of Catalase. The brain homogenate (100 μL) or 0.32 M sucrose was incubated with potassium phosphate buffer (2.25 mL, 65 mM) at pH 7.8 and 25 °C for 30 min. The reaction was initiated using 650 μL of hydrogen peroxide (7.5 mM), and the change in absorbance was measured at 240 nm for 2−3 min (UV, Shimadzu, Japan).[50]

3.6.4. Lipid Peroxide Assay. Lipid peroxidation was determined in terms of the thiobarbituric acid reactive substances (TBARS) content following the standard protocol by Ohkawa et al.[51] The reaction mixture consisting of 0.5 mL of brain homogenate, 1.5 mL of 0.9% aqueous solution of thiobarbituric acid (TBA), and 0.2 mL of 8% sodium dodecyl sulfate was incubated at 60 °C for 30 min. Once cooled, the red chromogen was extracted with 5 mL of a 15:1 v/v combination of *n*-butanol and pyridine, followed by 10 min of centrifugation at 4000 rpm. The absorbance of the organic layer was measured at 532 nm (UV, Shimadzu, Japan). In the 80−240 nmol concentration range, 1,1,3,3-tetra ethoxy propane was utilized as an external standard.

https://doi.org/10.1021/acsomega.2c07521
ACS Omega 2023, 8, 6825−6837

3.7. Protein Expression Studies Using Western Blot. The expressions of both PGC1-α and PPAR-γ upon treatment with the synthesized glitazones G1, G2, and pioglitazone (standard drug) were analyzed by western blotting. The neuronal cells from the brain sections of MPTP-induced mice, treated with varying concentrations of G1 and G2, were lysed with lysis buffer and centrifuged, and the supernatant layer was gathered. The sodium dodecyl sulfate-polyacrylamide gel electrophoresis (SDS-PAGE) was run at 200 V for 45−60 min, followed by the western blot analysis.

3.8. Histopathological Studies. The histopathological evaluation involved crystal violet staining of five-micron thick paraffin sections through matching coronal levels of the SNpc, which were observed under light microscopy at 100× magnification.

3.8.1. Estimation of the Neurotransmitter Dopamine. Dopamine level was quantified as per the procedure in the literature.[52,53] Briefly, the brain's hippocampal region was collected and homogenized with 0.5 M ice-cold high-performance liquid chromatography (HPLC)-grade methanol and then centrifuged at 15 000 rpm at −40 °C for 15 min. The supernatant was filtered using a 0.45 m membrane filter and stored at −80 °C until usage. Filtered supernatant (10 μL) was injected into the HPLC system to quantify at 1 mL/min flow of acetonitrile and phosphate dihydrogen phosphate using the C18 column by gradient elution technique. The signals for dopamine and MPTP were detected at 250 and 280 nm, respectively. Dopamine was quantified in terms of μg/g.

3.9. Statistical Analysis. One-way analysis of variance (ANOVA) was used in the statistical analysis, coupled with TUKEY post hoc, as multiple comparisons between groups. The results are expressed as mean ± standard deviation (SD) and analyzed by Graph pad Prism 8 software and SPSS version 17. Probability values of p less than 0.05 were deemed significant, whereas p values less than 0.001 were regarded as statistically significant.

4. CONCLUSION

The study illustrated the design and synthesis of novel glitazones G1 and G2 by targeting the PPAR-γ-dependent PGC-1α signaling in neurons and exhibiting dose-dependent neuroprotective activity comparable to the standard pioglitazone. The synthesized compounds exhibited significant neuroprotection, as reflected in the cell viability assay in LPS-induced SHSY5Y neuroblastoma cell lines. The neurobiochemical estimation of other antioxidant enzymes, SOD, GSH, and CAT, further ascertained these novel glitazones' free radical scavenging properties. The compounds successfully prevented MPTP-induced motor impairment, further establishing their neuroprotective role. The histopathological analysis revealed a reduction of degenerated neurons in the brain of the glitazones-treated mice. Similarly, dopamine levels were restored in MPTP-treated animals on treatment with G1 and G2. The study provides promising results demonstrating that G1 and G2 could serve as lead molecules in treating PD by focusing on the activation of PGC-1α signaling in neurons via PPAR-γ agonism. Extensive research on functional targets and signaling pathways in the processes is recommended to substantiate the findings further.

ASSOCIATED CONTENT

Supporting Information

The Supporting Information is available free of charge at https://pubs.acs.org/doi/10.1021/acsomega.2c07521.

Spectral data of G1 and G2, Raw data of TR-FRET PPARγ protein binding assay, HPLC results data, Grouping and treatment details of MPTP mice model of PD, Histopathology of acute oral toxicity (PDF)

AUTHOR INFORMATION

Corresponding Author

Prashantha Kumar BR − *Department of Pharmaceutical Chemistry, JSS College of Pharmacy, JSS Academy of Higher Education & Research, Mysuru 570 015 Karnataka, India;* orcid.org/0000-0001-9503-741X; Phone: +91-821-2548026; Email: brprashanthkumar@jssuni.edu.in; Fax: +91-821-2548359

Authors

Prabitha Prabhakaran − *Department of Pharmaceutical Chemistry, JSS College of Pharmacy, JSS Academy of Higher Education & Research, Mysuru 570 015 Karnataka, India*

Abhishek Nadig − *Department of Pharmacology, JSS College of Pharmacy, JSS Academy of Higher Education & Research, Mysuru 570 015 Karnataka, India*

Sahyadri M − *Department of Pharmacology, JSS College of Pharmacy, JSS Academy of Higher Education & Research, Mysuru 570 015 Karnataka, India*

Sunanda Tuladhar − *Department of Pharmacology, JSS College of Pharmacy, JSS Academy of Higher Education & Research, Mysuru 570 015 Karnataka, India*

Ruby Mariam Raju − *Department of Pharmaceutical Chemistry, JSS College of Pharmacy, JSS Academy of Higher Education & Research, Mysuru 570 015 Karnataka, India*

Saravana Babu Chidambaram − *Department of Pharmacology, JSS College of Pharmacy, JSS Academy of Higher Education & Research, Mysuru 570 015 Karnataka, India*

Bettadaiah Bheemanakere Kempaiah − *Spice and Flavour Science Department, CSIR-Central Food Technological Research Institute, Mysore 570 020 Karnataka, India*

Nulgumnalli Manjunathaiah Raghavendra − *Department of Pharmaceutical Sciences, Dayananda Sagar University, Bengaluru 560 078 Karnataka, India;* orcid.org/0000-0002-0846-012X

Complete contact information is available at: https://pubs.acs.org/10.1021/acsomega.2c07521

Notes

The authors declare no competing financial interest.

ACKNOWLEDGMENTS

One of the authors, Prabitha P., would like to thank the Department of Science and Technology (DST), Government of India, for the financial support under Women Scientist Scheme, WOS-A (File No. SR/WOS-A/CS-100/2018). The authors extend their appreciation to Principal, JSS College of Pharmacy, JSS Academy of Higher Education and Research, Mysore, for providing the opportunity to work on a project.

■ ABBREVIATIONS

ADMET, absorption, distribution, metabolism, excretion and toxicity; CAT, catalase; GSH, glutathione; GST, glutathione S-transferase; MP, Mucuna pruriens; MPTP, 1-methyl-4-phenyl-1,2,3,6-tetrahydropyridine; MTT, 3-[4,5-dimethylthiazol-2-yl]-2,5 diphenyl tetrazolium bromide; iNOS, inducible nitric oxide synthase; PBS, phosphate-buffered saline; PD, Parkinson's disease; PGC1-α, proliferator-activated receptor gamma coactivator 1-alpha; PPAR-γ, peroxisome proliferator-activated receptors gamma; RMSD, root-mean-square deviation; SOD, superoxide dismutase; SASA, solvent accessible surface area; TBARS, Thiobarbituric acid reactive substances; TR-FRET, time-resolved fluorescence resonance energy transfer

■ REFERENCES

(1) Pringsheim, T.; Jette, N.; Frolkis, A.; Steeves, T. D. L. The Prevalence of Parkinson's Disease: A Systematic Review and Meta-Analysis. *Movement Disorders* **2014**, *29* (13), 1583−1590.

(2) Rai, S. N.; Chaturvedi, V. K.; Singh, P.; Singh, B. K.; Singh, M. P. *Mucuna pruriens* in Parkinson's and in some other diseases: recent advancement and future prospective. *3 Biotech* **2020**, *10* (12), 522.

(3) Lehtonen, Š.; Sonninen, T. M.; Wojciechowski, S.; Goldsteins, G.; Koistinaho, J. Dysfunction of Cellular Proteostasis in Parkinson's Disease. *Front Neurosci* **2019**, *13* (5), 457.

(4) Pang, S. Y. Y.; Ho, P. W. L.; Liu, H. F.; Leung, C. T.; Li, L.; Chang, E. E. S.; Ramsden, D. B.; Ho, S. L. The Interplay of Aging, Genetics and Environmental Factors in the Pathogenesis of Parkinson's Disease. *Transl. Neurodegener.* **2019**, *8* (1). DOI: 10.1186/s40035-019-0165-9.

(5) Singleton, A.; Hardy, J. Progress in the Genetic Analysis of Parkinson's Disease. *Hum. Mol. Genet.* **2019**, *28* (R2), R215−R218.

(6) Rai, S. N.; Birla, H.; Singh, S. S.; Zahra, W.; Patil, R. R.; Jadhav, J. P.; Gedda, M. R.; Singh, S. P. Mucuna Pruriens Protects against MPTP Intoxicated Neuroinflammation in Parkinson's Disease through NF-KB/PAKT Signaling Pathways. *Front. Aging Neurosci.* **2017**, *9* (DEC). DOI: 10.3389/fnagi.2017.00421.

(7) Rai, S. N.; Birla, H.; Zahra, W.; Singh, S. S.; Singh, S. P. Immunomodulation of Parkinson's Disease Using Mucuna Pruriens (Mp). *J. Chem. Neuroanat* **2017**, *85*, 27−35.

(8) Carta, A. R.; Frau, L.; Pisanu, A.; Wardas, J.; Spiga, S.; Carboni, E. Rosiglitazone Decreases Peroxisome Proliferator Receptor-γ Levels in Microglia and Inhibits TNF-α Production: New Evidences on Neuroprotection in a Progressive Parkinson's Disease Model. *Neuroscience* **2011**, *194*, 250−261.

(9) Chaturvedi, R. K.; Beal, M. F. PPAR: A Therapeutic Target in Parkinson's Disease. *J. Neurochem* **2008**, *106* (2), 506−518.

(10) Landreth, G.; Jiang, Q.; Mandrekar, S.; Heneka, M. PPARgamma Agonists as Therapeutics for the Treatment of Alzheimer's Disease. *Neurotherapeutics* **2008**, *5* (3), 481−489.

(11) Nicolakakis, N.; Aboulkassim, T.; Ongali, B.; Lecrux, C.; Fernandes, P.; Rosa-Neto, P.; Tong, X. K.; Hamel, E. Complete Rescue of Cerebrovascular Function in Aged Alzheimer's Disease Transgenic Mice by Antioxidants and Pioglitazone, a Peroxisome Proliferator-Activated Receptor Gamma Agonist. *J. Neurosci.* **2008**, *28* (37), 9287−9296.

(12) Collino, M.; Patel, N. S. A.; Thiemermann, C. PPARs as New Therapeutic Targets for the Treatment of Cerebral Ischemia/Reperfusion Injury. *Ther Adv. Cardiovasc Dis* **2008**, *2* (3), 179−197.

(13) Kiaei, M.; Kipiani, K.; Chen, J.; Calingasan, N. Y.; Beal, M. F. Peroxisome Proliferator-Activated Receptor-Gamma Agonist Extends Survival in Transgenic Mouse Model of Amyotrophic Lateral Sclerosis. *Exp. Neurol.* **2005**, *191* (2), 331−336.

(14) Dehmer, T.; Heneka, M. T.; Sastre, M.; Dichgans, J.; Schulz, J. B. Protection by Pioglitazone in the MPTP Model of Parkinson's Disease Correlates with I Kappa B Alpha Induction and Block of NF Kappa B and INOS Activation. *J. Neurochem* **2004**, *88* (2), 494−501.

(15) Hunter, R. L.; Dragicevic, N.; Seifert, K.; Choi, D. Y.; Liu, M.; Kim, H. C.; Cass, W. A.; Sullivan, P. G.; Bing, G. Inflammation Induces Mitochondrial Dysfunction and Dopaminergic Neurodegeneration in the Nigrostriatal System. *J. Neurochem* **2007**, *100* (5), 1375−1386.

(16) Casper, D.; Yaparpalvi, U.; Rempel, N.; Werner, P. Ibuprofen Protects Dopaminergic Neurons against Glutamate Toxicity in Vitro. *Neurosci. Lett.* **2000**, *289* (3), 201−204.

(17) Kreisler, A.; Gelé, P.; Wiart, J. F.; Lhermitte, M.; Destée, A.; Bordet, R. Lipid-Lowering Drugs in the MPTP Mouse Model of Parkinson's Disease: Fenofibrate Has a Neuroprotective Effect, Whereas Bezafibrate and HMG-CoA Reductase Inhibitors Do Not. *Brain Res.* **2007**, *1135* (1), 77−84.

(18) Iwashita, A.; Muramatsu, Y.; Yamazaki, T.; Muramoto, M.; Kita, Y.; Yamazaki, S.; Mihara, K.; Moriguchi, A.; Matsuoka, N. Neuroprotective Efficacy of the Peroxisome Proliferator-Activated Receptor δ-Selective Agonists in Vitro and in Vivo. *Journal of Pharmacology and Experimental Therapeutics* **2007**, *320* (3), 1087−1096.

(19) Hunter, R. L.; Choi, D. Y.; Ross, S. A.; Bing, G. Protective Properties Afforded by Pioglitazone against Intrastriatal LPS in Sprague-Dawley Rats. *Neurosci. Lett.* **2008**, *432* (3), 198−201.

(20) Quinn, P. M. J.; Moreira, P. I.; Ambrósio, A. F.; Alves, C. H. PINK1/PARKIN Signalling in Neurodegeneration and Neuroinflammation. *Acta Neuropathol Commun.* **2020**, *8* (1), 189.

(21) Xing, B.; Liu, M.; Bing, G. Neuroprotection with Pioglitazone against LPS Insult on Dopaminergic Neurons May Be Associated with Its Inhibition of NF-KappaB and JNK Activation and Suppression of COX-2 Activity. *J. Neuroimmunol* **2007**, *192* (1−2), 89−98.

(22) Kurkowska-Jastrzębska, I.; Babiuch, M.; Joniec, I.; Przybyłkowski, A.; Członkowski, A.; Członkowska, A. Indomethacin Protects against Neurodegeneration Caused by MPTP Intoxication in Mice. *Int. Immunopharmacol* **2002**, *2* (8), 1213−1218.

(23) Jung, T. W.; Lee, J. Y.; Shim, W. S.; Kang, E. S.; Kim, S. K.; Ahn, C. W.; Lee, H. C.; Cha, B. S. Rosiglitazone Protects Human Neuroblastoma SH-SY5Y Cells against Acetaldehyde-Induced Cytotoxicity. *Biochem. Biophys. Res. Commun.* **2006**, *340* (1), 221−227.

(24) Jung, T. W.; Lee, J. Y.; Shim, W. S.; Kang, E. S.; Kim, S. K.; Ahn, C. W.; Lee, H. C.; Cha, B. S. Rosiglitazone Protects Human Neuroblastoma SH-SY5Y Cells against MPP+ Induced Cytotoxicity via Inhibition of Mitochondrial Dysfunction and ROS Production. *J. Neurol Sci.* **2007**, *253* (1−2), 53−60.

(25) Xing, B.; Xin, T.; Hunter, R. L.; Bing, G. Pioglitazone Inhibition of Lipopolysaccharide-Induced Nitric Oxide Synthase Is Associated with Altered Activity of P38 MAP Kinase and PI3K/Akt. *J. Neuroinflammation* **2008**, *5*, 4.

(26) Brakedal, B.; Flønes, I.; Reiter, S. F.; Torkildsen, Øi.; Dolle, C.; Assmus, J.; Haugarvoll, K.; Tzoulis, C. Glitazone Use Associated with Reduced Risk of Parkinson's Disease. *Mov. Disord.* **2017**, *32* (11), 1594−1599.

(27) Mäkelä, J.; Tselykh, T. v.; Kukkonen, J. P.; Eriksson, O.; Korhonen, L. T.; Lindholm, D. Peroxisome Proliferator-Activated Receptor-γ (PPARγ) Agonist Is Neuroprotective and Stimulates PGC-1α Expression and CREB Phosphorylation in Human Dopaminergic Neurons. *Neuropharmacology* **2016**, *102*, 266−275.

(28) Lee, E. Y.; Lee, J. E.; Park, J. H.; Shin, I. C.; Koh, H. C. Rosiglitazone, a PPAR-γ Agonist, Protects against Striatal Dopaminergic Neurodegeneration Induced by 6-OHDA Lesions in the Substantia Nigra of Rats. *Toxicol. Lett.* **2012**, *213* (3), 332−344.

(29) Patrone, C.; Eriksson, O.; Lindholm, D. Diabetes Drugs and Neurological Disorders: New Views and Therapeutic Possibilities. *Lancet Diabetes Endocrinol* **2014**, *2* (3), 256−262.

(30) Swanson, C. R.; Joers, V.; Bondarenko, V.; Brunner, K.; Simmons, H. A.; Ziegler, T. E.; Kemnitz, J. W.; Johnson, J. A.; Emborg, M. E. The PPAR-γ Agonist Pioglitazone Modulates Inflammation and Induces Neuroprotection in Parkinsonian Monkeys. *J. Neuroinflammation* **2011**, *8*. DOI: 10.1186/1742-2094-8-91.

(31) Jarrar, M. H.; Baranova, A. PPARγ Activation by Thiazolidinediones (TZDs) May Modulate Breast Carcinoma Out-

https://doi.org/10.1021/acsomega.2c07521
ACS Omega 2023, 8, 6825−6837

come: The Importance of Interplay with TGFβ Signalling. *J. Cell Mol. Med.* **2007**, *11* (1), 71.
(32) Berrouet, C.; Dorilas, N.; Rejniak, K. A.; Tuncer, N. Comparison of Drug Inhibitory Effects (IC50) in Monolayer and Spheroid Cultures. *Bull. Math Biol.* **2020**, *82* (6), 68.
(33) Yadav, S. K.; Rai, S. N.; Singh, S. P. Mucuna Pruriens Reduces Inducible Nitric Oxide Synthase Expression in Parkinsonian Mice Model. *J. Chem. Neuroanat* **2017**, *80*, 1−10.
(34) Singh, S. S.; Rai, S. N.; Birla, H.; et al. Effect of Chlorogenic Acid Supplementation in MPTP-Intoxicated Mouse. *Front Pharmacol.* **2018**, *9*, 757.
(35) Chang, Y. H.; Yen, S. J.; Chang, Y. H.; Wu, W. J.; Lin, K. D. Pioglitazone and Statins Lower Incidence of Parkinson Disease in Patients with Diabetes Mellitus. *Eur. J. Neurol* **2021**, *28* (2), 430−437.
(36) Zahra, W.; Rai, S. N.; Birla, H.; et al. Neuroprotection of Rotenone-Induced Parkinsonism by Ursolic Acid in PD Mouse Model. *CNS Neurol Disord Drug Targets.* **2020**, *19* (7), 527−540.
(37) Iarkov, A.; Barreto, G. E.; Grizzell, J. A.; Echeverria, V. Strategies for the Treatment of Parkinson's Disease: Beyond Dopamine. *Front Aging Neurosci* **2020**, *12*, 4.
(38) Ewing, T. J. A.; Makino, S.; Skillman, A. G.; Kuntz, I. D. DOCK 4.0: Search Strategies for Automated Molecular Docking of Flexible Molecule Databases. *J. Comput. Aided Mol. Des* **2001**, *15* (5), 411−428.
(39) Wu, G.; Robertson, D. H.; Brooks, C. L.; Vieth, M. Detailed Analysis of Grid-Based Molecular Docking: A Case Study of CDOCKER - A CHARMm-Based MD Docking Algorithm. *J. Comput. Chem.* **2003**, *24* (13), 1549−1562.
(40) Wu, X.; Milne, J. L. S.; Borgnia, M. J.; Rostapshov, A. V.; Subramaniam, S.; Brooks, B. R. A Core-Weighted Fitting Method for Docking Atomic Structures into Low-Resolution Maps: Application to Cryo-Electron Microscopy. *J. Struct Biol.* **2003**, *141* (1), 63−76.
(41) Li, Y.; Kovach, A.; Suino-Powell, K.; Martynowski, D.; Xu, H. E. Structural and Biochemical Basis for the Binding Selectivity of Peroxisome Proliferator-Activated Receptor γ to PGC-1α. *J. Biol. Chem.* **2008**, *283* (27), 19132−19139.
(42) Wang, T.; Brudvig, G. W.; Batista, V. S. Study of Proton Coupled Electron Transfer in a Biomimetic Dimanganese Water Oxidation Catalyst with Terminal Water Ligands. *J. Chem. Theory Comput* **2010**, *6* (8), 2395−2401.
(43) Mark, P.; Nilsson, L. Structure and Dynamics of the TIP3P, SPC, and SPC/E Water Models at 298 K. *J. Phys. Chem. A* **2001**, *105* (43), 9954−9960.
(44) National Research Council (US) Institute for Laboratory Animal Research. *Guide for the Care and Use of Laboratory Animals;* National Academies Press (US), 1996. DOI: 10.17226/5140.
(45) OECD guideline for testing of chemicals. *The Organization of Economic Co-Operation and Development Guidelines Test No. 423: Acute Oral Toxicity - Acute Toxic Class Method, OECD Guidelines for the Testing of Chemicals, Section 4;* OECD, 2002.
(46) Woodlee, M. T.; Schallert, T. The Impact of Motor Activity and Inactivity on the Brain: Implications for the Prevention and Treatment of Nervous-System Disorders. *Curr. Dir Psychol Sci.* **2006**, *15* (4), 203−206.
(47) Kresge, N.; Simoni, R. D.; Hill, R. L. The Most Highly Cited Paper in Publishing History: Protein Determination by Oliver H. Lowry. *J. Biol. Chem.* **2005**, *280* (28), e26−e28.
(48) Lowry, O. H.; Rosebrough, N. J.; Farr, A. L.; Randall, R. J. Protein Measurement with the Folin Phenol Reagent. *J. Biol. Chem.* **1951**, *193* (1), 265−275.
(49) Jollow, D.; Mitchell, J. R.; Zampaglione, N.; Gillette, J. R. Bromobenzene-Induced Liver Necrosis. Protective Role of Glutathione and Evidence for 3,4-Bromobenzene Oxide as the Hepatotoxic Metabolite. *Pharmacology* **1974**, *11* (3), 151−169.
(50) Beers, R. F.; Sizer, I. W. A Spectrophotometric Method for Measuring the Breakdown of Hydrogen Peroxide by Catalase. *J. Biol. Chem.* **1952**, *195* (1), 133−140.
(51) Ohkawa, H.; Ohishi, N.; Yagi, K. Assay for lipid peroxides in animal tissues by thiobarbituric acid reaction. *Anal. Biochem.* **1979**, *95* (2), 351−358.
(52) Yang, L.; Beal, M. F. Determination of Neurotransmitter Levels in Models of Parkinson's Disease by HPLC-ECD. *Methods Mol. Biol.* **2011**, *793*, 401−415.
(53) Lu, J.; Sun, F.; Ma, H.; Qing, H.; Deng, Y. Quantitative Detection of Dopamine, Serotonin and Their Metabolites in Rat Model of Parkinson's Disease Using HPLC-MS/MS. In *2015 IEEE International Conference on Mechatronics and Automation, ICMA 2015;* IEEE, 2015; pp 1460−1465. DOI: 10.1109/ICMA.2015.7237700.

https://doi.org/10.1021/acsomega.2c07521
ACS Omega 2023, 8, 6825−6837